

The Effect of Stress Arching on the Permeability Sensitive Experiment in the Su Lige Gas Field

Fanliao Wang¹, Xiangfang Li², Gary Couples³, Mingchuan Wang⁴, Yiqun Zhang⁵ and Jingjing Zhao⁶

¹ Laboratory of Petroleum Engineering in China University of Petroleum, Beijing, 102249, China

² Institute of Petroleum Engineering, Heriot-Watt University, Heriot-Watt University, Edinburgh, EH14 4AS, UK

³ Civil and environmental engineering school, University of Science and Technology Beijing, Beijing, 100083, China.

⁴ The company production of Jiangsu Oilfield Branch Factory of Formosa Petrochemical Co in China, Yangzhou, 225264, China

E-mail: wangfanliao@163.com

Abstract. Comparing with the high permeability reservoir, low permeability reservoir was more sensitive to the effective stress and current stress sensitive experiment assumed that the overburden pressure unchanged during the production. In fact, the overburden pressure reduced during the production due to the stress arching effect and it is easy to form an arch in the overburden when the reservoir was small and softer than the surrounding rock. Based on the theory of stress arch, Arching ratios and overburden pressures in the Su Lige gas field were calculated and this theory was the first time to be applied in the stress sensitive experiments. The experiments considered the shapes of the reservoirs. The shapes of the reservoirs in the Su Lige gas field were classified as the Penny shape and the Elliptic cylinder reservoirs. The arching ratios were 0.12 and 0.28, respectively, for the Elliptic cylinder reservoirs and the Penny shape reservoirs. The permeabilities with stress arch were much larger than those obtained from the routine experiments. The increase proportions of the permeability were related to the arching ratios. The permeabilities increased by 23% and 50%, respectively, for the Elliptic cylinder reservoir and the Penny- shape reservoir with the pressure drop of 25Mpa. The routine sensitive experiments exaggerated the degree of permeability stress sensitivity.

1. Introduction

Rock permeability is sensitive to the effective stress and Current stress sensitive experiments assume that the overburden pressure is a constant during the production [1-3]. However, the non-uniform distribution of the pore pressure leads to stress arches formed in the overburden. Part weight of the overburden is transformed to the sideburden through the arch and the overburden pressure reduces during the production [4-9]. Stress arching ratio is used to describe the degree of the stress arch and it is related to the geometry and rock properties of the reservoir and surrounding rock It is easy to form an arch in the overburden when the reservoir is small and the strength of the reservoir rock is softer than that of the surrounding rock [8-9].

In this paper, two kinds of reservoir model are established based on the geological data in the Su Lige gas field. Stress arching ratios and overburden pressure are calculated using the theory of the stress arch. A new stress sensitive experiment considering the stress arching effect was established.

2. Overburden Pressure Calculation considering Stress arching effect

In general case, the overburden pressure is calculated by Eq. (1).

$$\sigma_0 = \int_0^z \{ [1 - \phi(z)] \rho_G(z) + \phi(z) \rho_f(z) \} g dz \quad (1)$$

¹ Corresponding author

where, z is the reservoir depth, m; $\varphi(z)$, $\rho_G(z)$, $\rho_f(z)$ are, respectively, rock porosity, rock density and fluid density at the depth of z , kg/m³; g is the gravity acceleration, 9.8m/s²; σ_0 is the overburden pressure, which is always assumed to be unchanged during the production. In fact, the overburden pressure changes when an arch forms in the overburden, and the stress change is related to the stress arching ratio and pore pressure change [5-7].

$$\Delta\sigma = \gamma\alpha\Delta p \quad (2)$$

where, α is Biot's coefficient, which usually equals to 1 in the analysis [10]; ΔP is pressure change, which is negative for production but positive for injection, Mpa; γ is stress arching ratio. Then the overburden pressure and the effective stress are expressed by Eq. (3) and Eq. (4).

$$\sigma = \sigma_0 - \gamma\alpha\Delta p \quad (3)$$

$$\sigma' = \sigma_0 - \alpha p_0 - (\gamma - 1)\Delta p \quad (4)$$

where, P_0 is initial pore pressure, Mpa; ρ is the overburden pressure, Mpa; σ_0 is the initial overburden pressure, which is calculated by Eq. (1); σ' is the effective stress, Mpa.

Soltanzadeh and Hawkes [7] used the theories of inclusion and inhomogeneities to calculate the stress arching ratios of the reservoir with idealized geometries (See Table 1). The theories assumed that the reservoirs possessed elastic properties, uniform pressure change with deep depth. The theory of the inclusion was suitable to calculate arching ratio of the reservoir with the same rock properties as the surrounding's. However the theory of the inclusion was appropriate for the reservoir with different rock properties from the surroundings'. To understand the theories, we need to know some important parameters. μ^* , μ are respective the shear modules of the reservoir and surroundings, Gpa. And ν^* , ν are the Poisson's ratios respective for the reservoir and surroundings; $R\mu$ is the ratio of the reservoir's shear modulus and the surrounding rock's; e is the ratio of the thickness and the width of the reservoir, which is called aspect ratio.

The stress arching ratios increased with the increasing of the aspect ratios but decreased with the increasing of the Poisson's ratio and shear module ratio of the reservoir. The effect of the Poisson's ratio of the surroundings on the arching ratio could be neglected [8, 9]. It is much easier to form an arch in the overburden in the soft reservoir with large aspect ratio, small Poisson's ratio.

3. Stress sensitive experiment with stress arching effect in Su Lige gas field

3.1. Experimental Apparatus

The experimental apparatus used to assess the permeability stress sensitivity was schematically shown in Figure 1.

3.2. Experimental Procedure

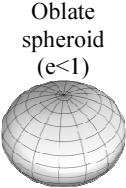



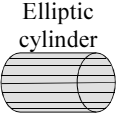
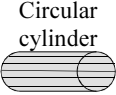
The key of the experiment was to reconstruct the condition similar to the situation during the production. The confining pressure represents the overburden pressure in the experiment.

Firstly, the sample were dried at 110°C, weighted, and then saturated with formation water to establish irreducible water saturation.

Secondly, the saturated core was placed in the core holder. And then establish the initial reservoir condition and remained it for 24 hours to in case of time effect.

Thirdly, the back pressure was reduced so that the differential pressure between upstream and downstream was 1.5~2Mpa and remained unchanged to prevent the existence of high-speed non-Darcy flow. The average fluid pressure was reduced by every 1Mpa and the confining pressure was adjusted using the result of the Equation (3), and the flow rate measures were carried out until the flow stayed steady.

Table 1. Stress arching ratios for different shape reservoirs using the theory of Inclusion and inhomogeneity.

Shape	Inclusion (Reservoir and surrounding rock have identical elastic properties)	Inhomogeneity (Elastic properties of the reservoir are different from the surrounding rock)
When the reservoir and the surrounding rock have the same Poisson's ratio:		
$\gamma = B_1 / B_2$, $B_1 = (1 + \nu)[1 - (R_\mu - 1)X_1 - X_2] + R_\mu[(1 - \nu)X_4 + 2\nu X_3]$, $B_2 = (1 + \nu)[(R_\mu - 1)^2 X_1 + (R_\mu - 1)X_2 + 1]$, $X_1 = (S_1 + S_2)S_5 - 2S_4S_3$, $X_2 = S_1 + S_2 + S_5$, $X_3 = S_5 - S_3$, $X_4 = S_1 + S_2 - 2S_4$, $F = 1 / (e^2 - 1) + (e \cos^{-1} e) / (1 - e^2)^{3/2}$,		
 <p>Oblate spheroid ($e < 1$)</p>	$\gamma = \frac{1 - 2\nu}{1 - \nu} \left[\frac{e \cos^{-1} e}{(1 - e^2)^{3/2}} - \frac{e^2}{1 - e^2} \right]$	$S_1 = \frac{3}{8(1 - \nu)} \left[1 - \frac{1 + 3F}{2(e^2 - 1)} \right] + \frac{1 - 2\nu}{4(1 - \nu)} (1 + F)$, $S_2 = \frac{1}{8(1 - \nu)} \left[1 - \frac{1 + 3F}{2(e^2 - 1)} \right] - \frac{1 - 2\nu}{4(1 - \nu)} (1 + F)$, $S_3 = \frac{1}{4(1 - \nu)} \frac{e^2 (1 + 3F)}{e^2 - 1} - \frac{1 - 2\nu}{4(1 - \nu)} (1 + F)$, $S_4 = \frac{1}{4(1 - \nu)} \frac{1 + 3F}{(e^2 - 1)} + \frac{1 - 2\nu}{2(1 - \nu)} F$, $S_5 = \frac{1}{2(1 - \nu)} \left[1 - \frac{e^2 (1 + 3F)}{(e^2 - 1)} \right] - \frac{1 - 2\nu}{2(1 - \nu)} F$
 <p>Prolate spheroid</p>	$\gamma = \frac{1 - 2\nu}{1 - \nu} \left[\frac{e^2}{e^2 - 1} - \frac{e \cosh^{-1} e}{(e^2 - 1)^{3/2}} \right]$	
 <p>Sphere</p>	$\gamma = \frac{2(1 - 2\nu)}{3(1 - \nu)}$	$\gamma = \frac{2(1 - 2\nu^*)}{R_\mu (1 + \nu^*) + 2(1 - 2\nu^*)}$
When the reservoir and the surrounding rock have the same Poisson's ratio:		
 <p>Penny shape</p>	$\gamma = \frac{1 - 2\nu}{1 - \nu} \frac{\pi e}{2}$	$\gamma = C_1 / C_2$ where, $C_1 = \pi e(1 - 2\nu) [\pi e(1 - R_\mu)(1 + \nu) - 2R_\mu(1 - 2\nu) - 2]$, $C_2 = (R_\mu - 1)\pi e \{ (1 - 2\nu)[2 - \pi e(1 - R_\mu)(1 + \nu)] - R_\mu(3 - 4\nu)(1 + \nu) \} - 8R_\mu(1 - \nu)^2$
 <p>Elliptic cylinder</p>	$\gamma = \frac{1 - 2\nu}{1 - \nu} \frac{e}{1 + e}$	$\gamma = A_1 / A_2$, $A_1 = (1 - 2\nu^*) \{ R_\mu [2e(1 - \nu) + 1 - 2\nu] + 1 \} e$, $A_2 = R_\mu [2(1 + e)^2 (1 - \nu)(1 - \nu^*) - 2e\nu^* (1 - 2\nu) + R_\mu e(3 - 4\nu)] + e(1 - 2\nu^*)$
 <p>Circular cylinder</p>	$\gamma = \frac{1}{2} \frac{1 - 2\nu}{1 - \nu}$	$\gamma = \frac{1 - 2\nu^*}{R_\mu + 1 - 2\nu^*}$
Infinite	$\gamma = 0$	$\gamma = 0$

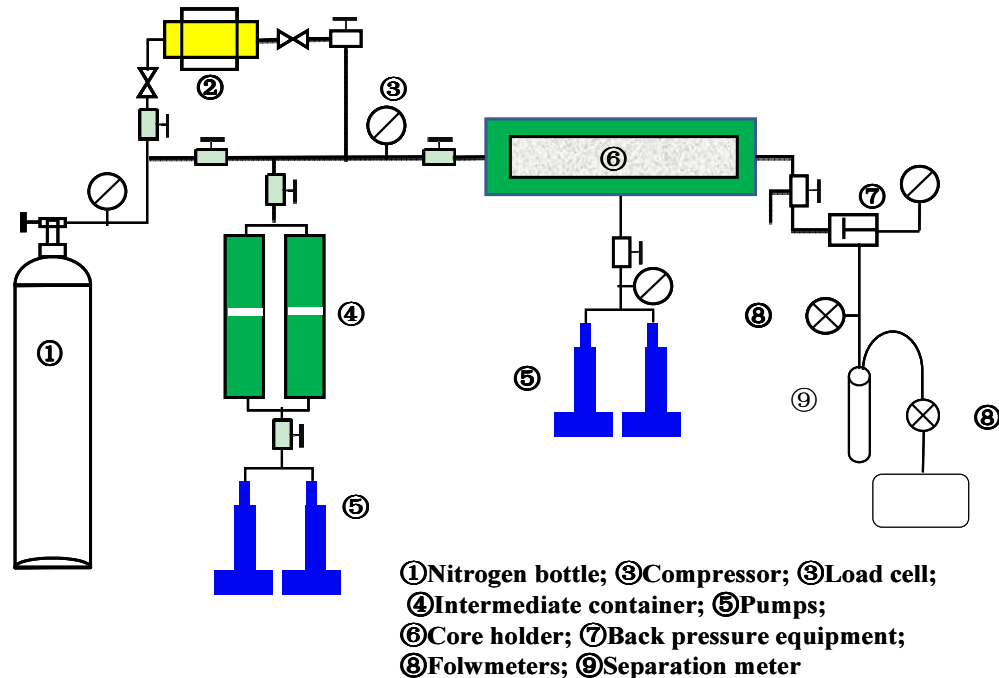


Figure 1. Experimental test apparatus.

All the tests were performed at a constant temperature of 25°C, and the gas was pure nitrogen. The permeability was calculated using the Darcy equation. Subsequently, the stress sensitive permeability was obtained for different pore pressure and overburden pressure.

3.3. Results and Discussion

The Su Lige gas field is located in the Ordos basin of China, and covers an area of 20000km². The field is a large sandstone lithological traps gas reservoir. He8 and Shan1 are the main production formations. The gas field belongs to braided river deposits. Statistics show that 75% of the effective sandstone is isolated, and most of the isolated sand is controlled by one well. The main shapes of the reservoir are elliptic cylinder reservoir and penny shape reservoir.

The main reservoir parameters are showed in Table 2. The initial overburden pressure was 62.22Mpa calculated by Eq. (1), the arching ratios are 0.12 and 0.28, respectively, for elliptic cylinder reservoir and penny shape reservoir.

Figure 2 illustrated the results for different arching ratios in the Su Lige gas field.

Fig. 2. and Fig. 3 showed that the permeabilities impacted by the stress arch. The permeabilities increased with the increasing of the stress arching ratio. The increase proportion was large with large number of stress arching ratio. The increase proportions were 23% and 50%, respectively, for the Elliptic cylinder reservoir and the Penny-shape reservoir. The routine core experiments exaggerated the influence of the permeability stress sensitivity. It should be noted that this study emphasizes the stress arching effect in the overburden rock and neglects the stress arches in the horizontal direction. If we consider the stress arches in both vertical and horizontal directions, the permeability increasing proportions are larger than that obtained only considering the arches in the vertical direction. And this problem can be solved if we consider the effect of the stress path, which was defined as the ratio of the horizontal effective stress and vertical effective stress during the production. Some authors have done experiments considering the stress path, but they still assumed that the vertical stress didn't change. Meanwhile, we believe that the theory of the stress arch will play an important role in the petroleum industry.

Table 2. Parameters of Su Lige gas field

Properties	Reservoir
Initial Pore pressure P_0 (Mpa)	31.01
Porosity φ	0.1
Depth H (m)	2980
Width W (m)	400
Thickness h (m)	10-80
Shear module ratio R_μ	0.75
Rock density ρ (cm ³ /d)	2.247
Possios ratio ν	0.2
Permeability K_i (mD)	0.1

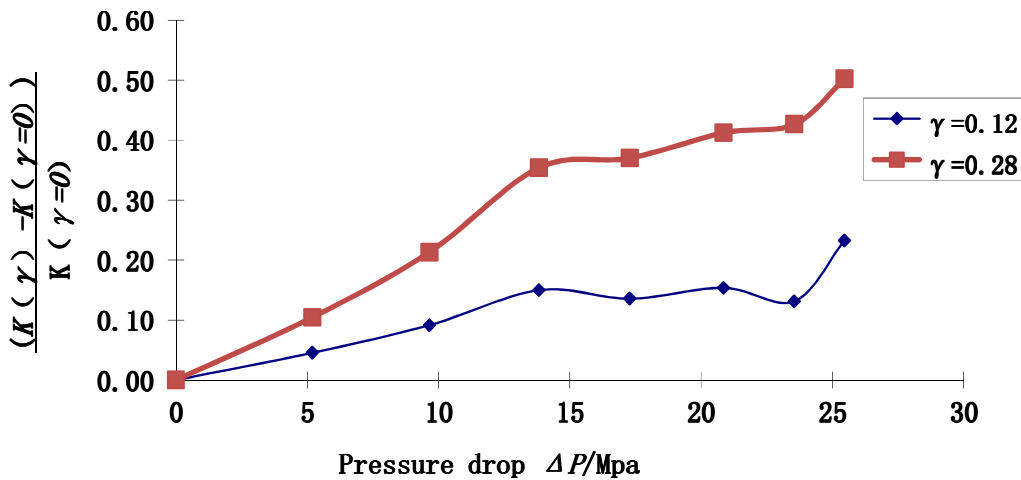


Figure 3. Permeability increasing proportion for different shape of the reservoirs.

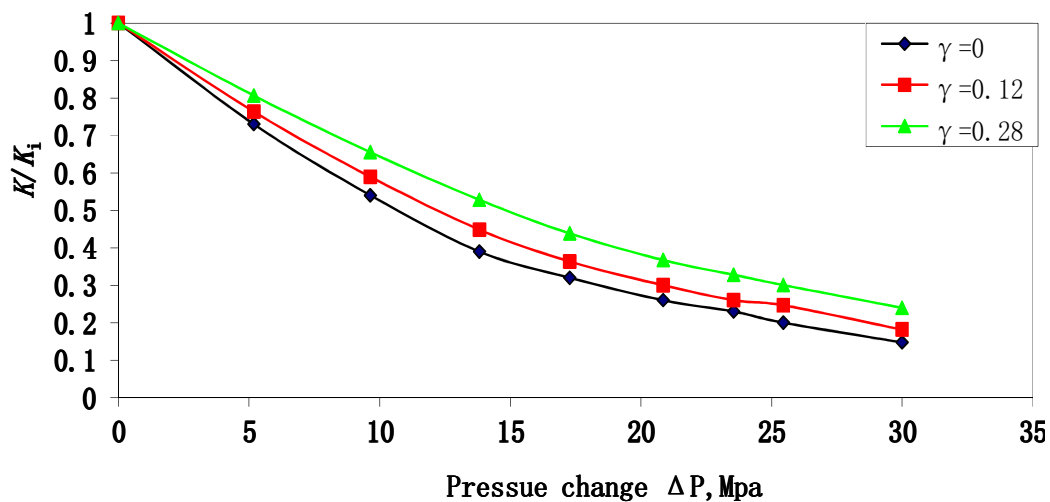


Figure 2. Normalized permeability for different shape of the reservoirs.

4. Conclusions

This study uncovered an important phenomenon-related stress arching effect during the production. Based on the theory of the stress arch, the overburden pressure was calculated and it was the first time to use this theory in the stress sensitive experiments. The shapes of the reservoirs in Su Lige gas field were classified as the Penney-shape reservoir and the Elliptic cylinder reservoir. The arching ratios were 0.12 and 0.28, respectively, for the Elliptic cylinder reservoir and the Penney-shape reservoir.

A new stress sensitive laboratory procedure with stress arch was presented. Cores with arch effect had larger permeability than those of routine experiments at the same condition. The permeability increase proportion was large with the big stress arch ratio. The increase proportions were 23% and 50%, respectively, for the Elliptic cylinder reservoir and the Penny-shape reservoir. The routine core experiment without the stress arching effect exaggerated the permeability sensitivity.

References

- [1] Rhett D W and Teufel D W 1996 Stress Dependence of Matrix Permeability of North Sea Sandstone Reservoir Rock *33rd U.S. Symposium on Rock Mechanics*, **345** 12–8
- [2] Holt R M 1990 Permeability Reduction Induced by a Non-hydrostatic Stress Field *SPE Formation Evaluation* **5(4)** 444–8
- [3] Dautriat J, Gland N, Guelard J, et al. 2009 Axial and Radial Permeability Evolutions of Compressed Sandstones: End Effects and Shear-band Induced Permeability Anisotropy *Pure and Applied Geophysics* **166(5–7)** 1037–61
- [4] Teufel L W, Rhett D W and Farrell H E 1991 Effect of Reservoir Depletion And Pore Pressure Drawdown On In Situ Stress And Deformation In the Ekofisk Field, North Sea *32nd U.S. Symposium on Rock Mechanics (USRMS)* 12–27
- [5] H Soltanzadeh, C D Hawkes and J Sharma 2007 Closed-form solutions for production- and injection-induced stresses in plane-strain reservoirs with elastic properties different from the surrounding rock *International Journal of Geomechanics* **7(5)** 353–61
- [6] Soltanzadeh H and Hawkes C D 2008 Semi-Analytical Models for Stress Change and Fault Reactivation Induced by Reservoir Production and Injection *Journal of Petroleum Science and Engineering* **60(2)** 71–85
- [7] Soltanzadeh H and Hawkes C D 2009 Induced Poroelastic and thermoelastic stress changes within reservoirs during fluid injection and production *Porous Media: Heat and Mass Transfer, Transport and Mechanics* 27–57
- [8] Dusseault M B 2011 Geomechanical challenges in petroleum reservoir exploitation *Journal of Civil Engineering* **15(4)** 669–78
- [9] Verdon J P Geomechanical simulation of CO₂ injection *Microseismic monitoring and geomechanical modelling of co₂ storage in subsurface reservoirs* 83–105
- [10] Biot M A and Willis D G 1957 The elastic coefficients of the theory of consolidation *ASME Journal of Applied Mechanics* **24(2)** 594–601.